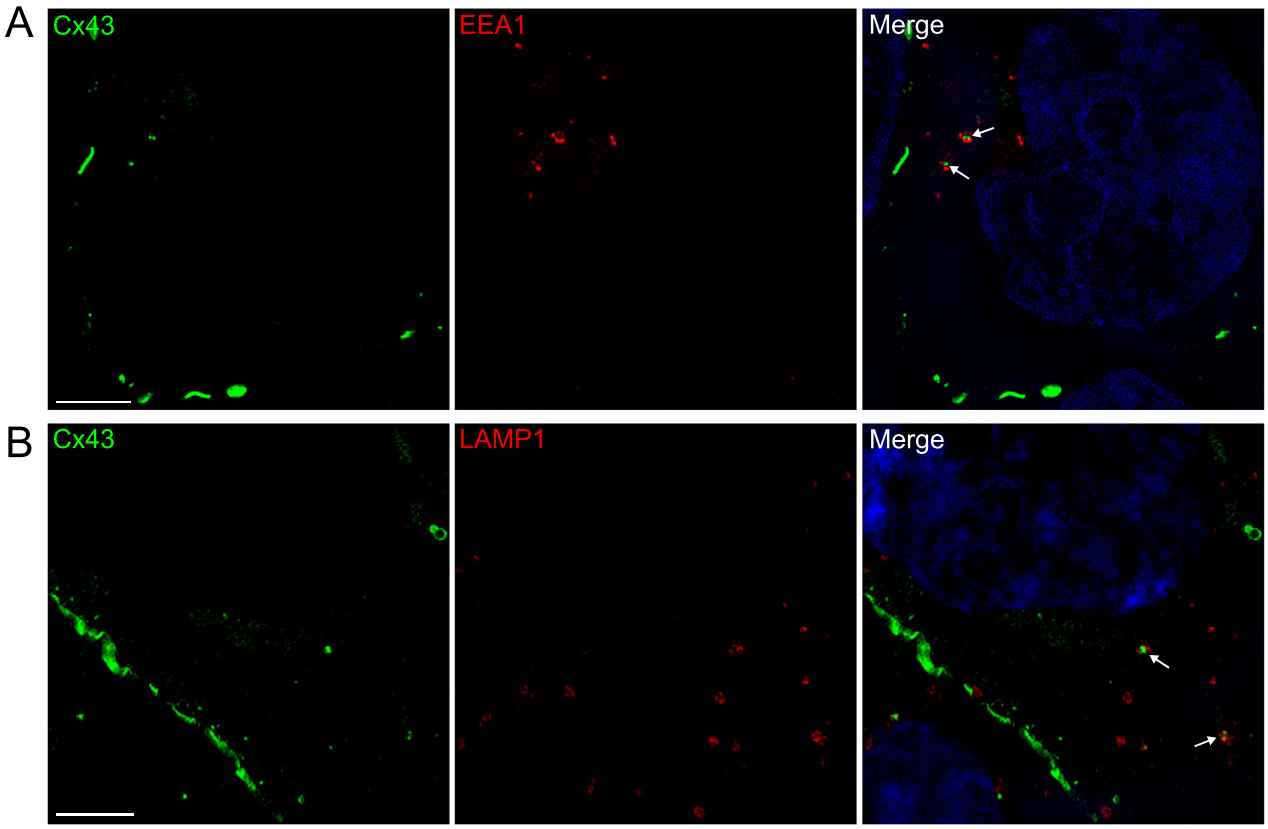

Supplementary Figure S1. Super-resolution microscopy analysis of the subcellular localization of Cx43 in HeLa-Cx43 cells. HeLa-Cx43 cells were fixed and stained with anti-Cx43 (green) in combination with either **(A)** anti-EEA1 (red) or **(B)** anti-LAMP1 (red) antibodies followed by Alexa488- and Alexa555-conjugated secondary antibodies. Nuclei were stained with Hoechst 33342 (blue). Cells were imaged by SIM. Arrows indicate localization of Cx43 in vesicular structures positive for EEA1 (A) or LAMP1 (B). Scale bar, 4 µm.

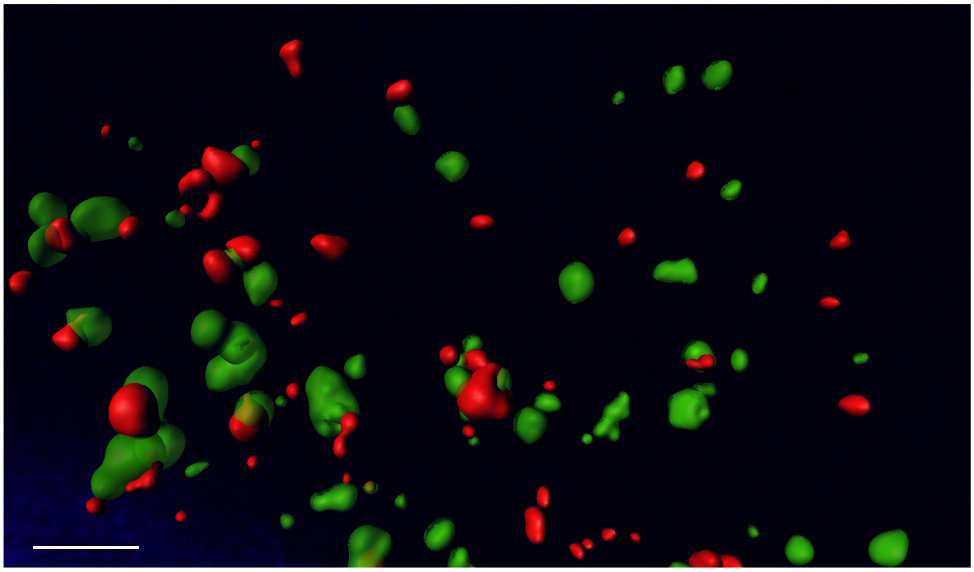

Supplementary Figure S2. Three-dimensional reconstruction of the subcellular localization of Cx43 and EEA1 in TPA-treated HeLa-Cx43 cells. HeLa-Cx43 cells were treated with TPA (100 ng/ml) for 90 minutes, fixed and stained with anti-Cx43 (green) and anti-EEA1 (red) antibodies followed by Alexa488- and Alexa555-conjugated secondary antibodies. Nuclei were stained with Hoechst 33342 (blue). Cells were imaged by SIM, and images were subjected to surface three-dimensional rendering using IMARIS. Scale bar, 1 µm.

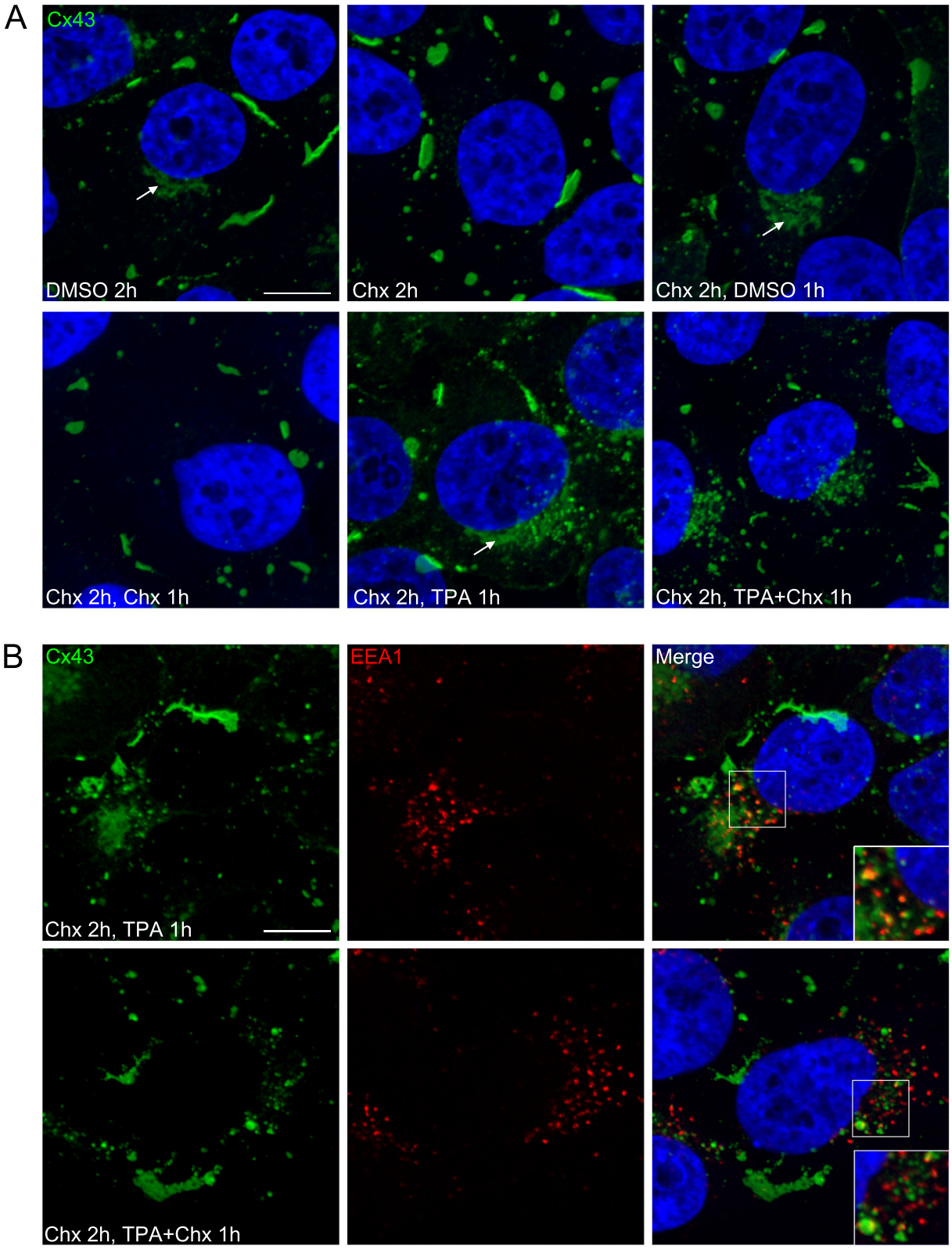

Supplementary Figure S3. Analysis of the subcellular localization of Cx43 in response to TPA treatment after preincubation with cycloheximide. (A) HeLa-Cx43 cells were treated with DMSO (solvent) or cycloheximide (Chx, 10 µM) for 2 hours, or preincubated with Chx (10 µM) for 2 hours followed by treatment with DMSO, Chx (10 µM), TPA (100 ng/ml) or Chx (10 µM) in combination with TPA (100 ng/ml) for 1 hour. Cx43 (green) was

analyzed by confocal microscopy. Arrows indicate diffuse perinuclear Cx43 staining, probably representing newly synthesized Cx43. Scale bar, 10 µm, applies to all images. **(B)** HeLa-Cx43 cells were preincubated with Chx (10 µM) for 2 hours followed by treatment with TPA (100 ng/ml) alone or with TPA (100 ng/ml) in combination with Chx for 1 hour. Cx43 (green) and EEA1 (red) were visualized by confocal microscopy. Scale bar, 10 µm, applies to all images.

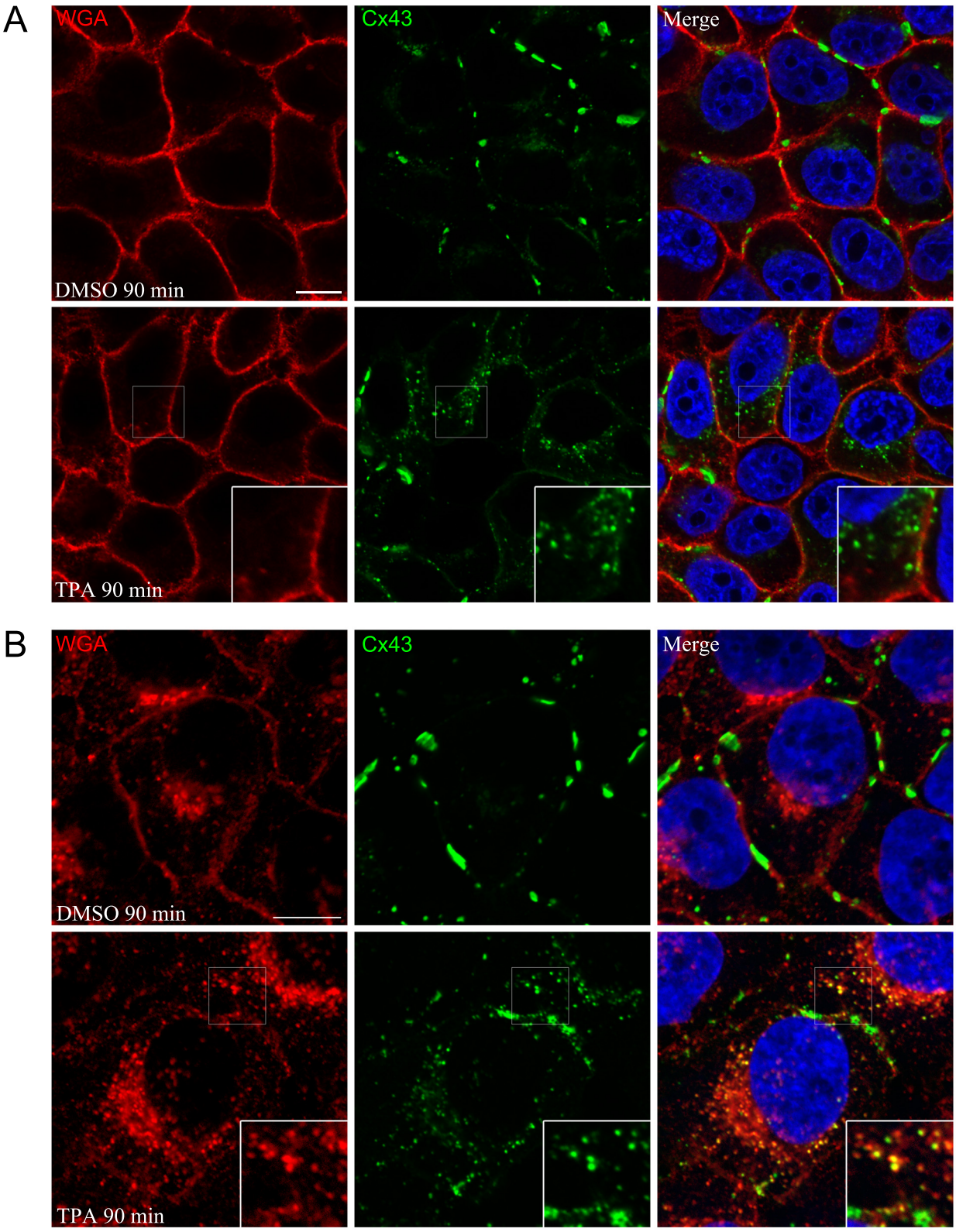

Supplementary Figure S4. Cx43 and WGA staining in HeLa-Cx43 cells. HeLa-Cx43 cells were **(A)** treated with either DMSO (solvent) or TPA (100 ng/ml) for 90 minutes and then incubated with Alexa555-conjugated WGA for 10 minutes to stain the plasma membrane or **(B)** incubated with Alexa555-conjugated WGA for 10 minutes to stain the plasma membrane and then treated with either DMSO (solvent) or TPA (100 ng/ml) for 90 minutes. Cx43 (green) and WGA (red) were visualized by confocal microscopy. Scale bars, 10 µm, apply to all images.

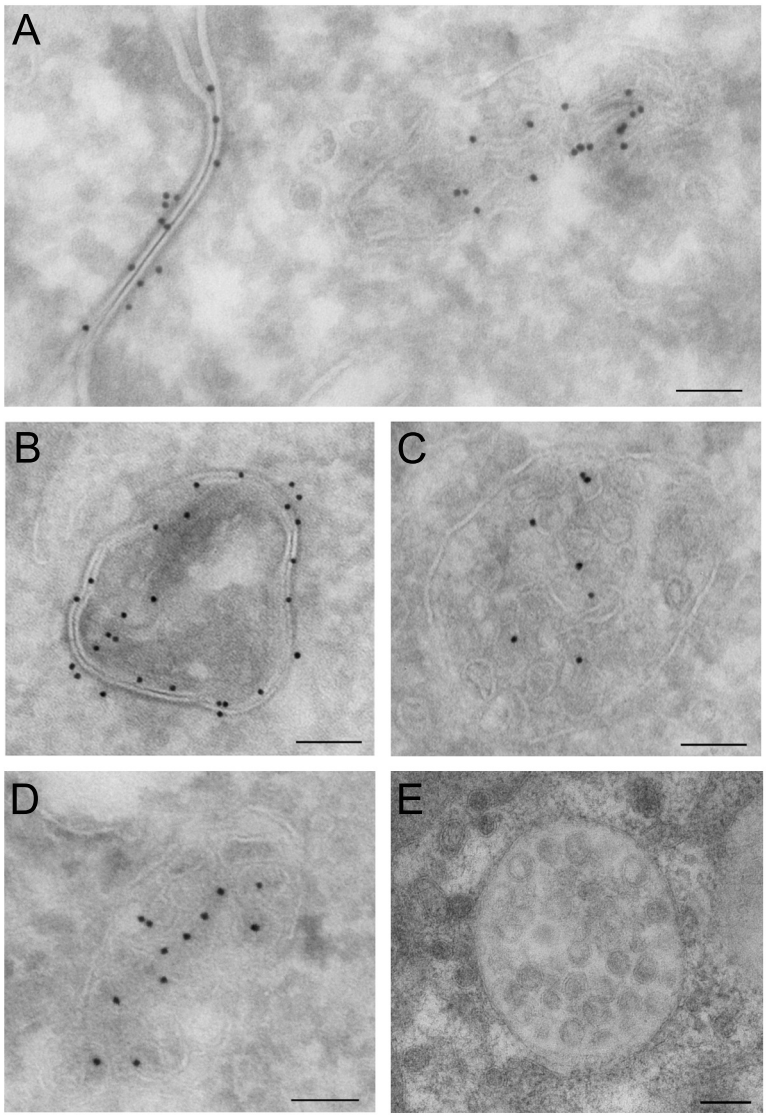

Supplementary Figure S5. Immunoelectron microscopy analysis of Cx43 localization in HeLa-Cx43 cells. Cells were left untreated **(A, D)** or treated with TPA (100 ng/ml) **(B, C)** for 60 minutes and fixed for immunoelectron microscopy. Ultrathin cryosections were labeled against Cx43 by using anti-Cx43 antibodies followed by incubation with 10 nm Protein A-gold particles. **(A)** Cx43 immunogold staining in a gap junction between two adjacent cells (left-hand side of the image) and in a multivesicular endosome (right-hand side of the image). **(B)** Cx43 immunogold staining in an annular gap junction. **(C, D)** Cx43 immunogold staining in multivesicular endosomes in TPA-treated **(C)** and untreated **(D)** HeLa-Cx43 cells. **(E)** For comparison, a multivesicular endosome as observed in cells that have been high-pressure frozen, freeze substituted, and embedded in Lowicryl, is shown. Scale bars, 100 nm.

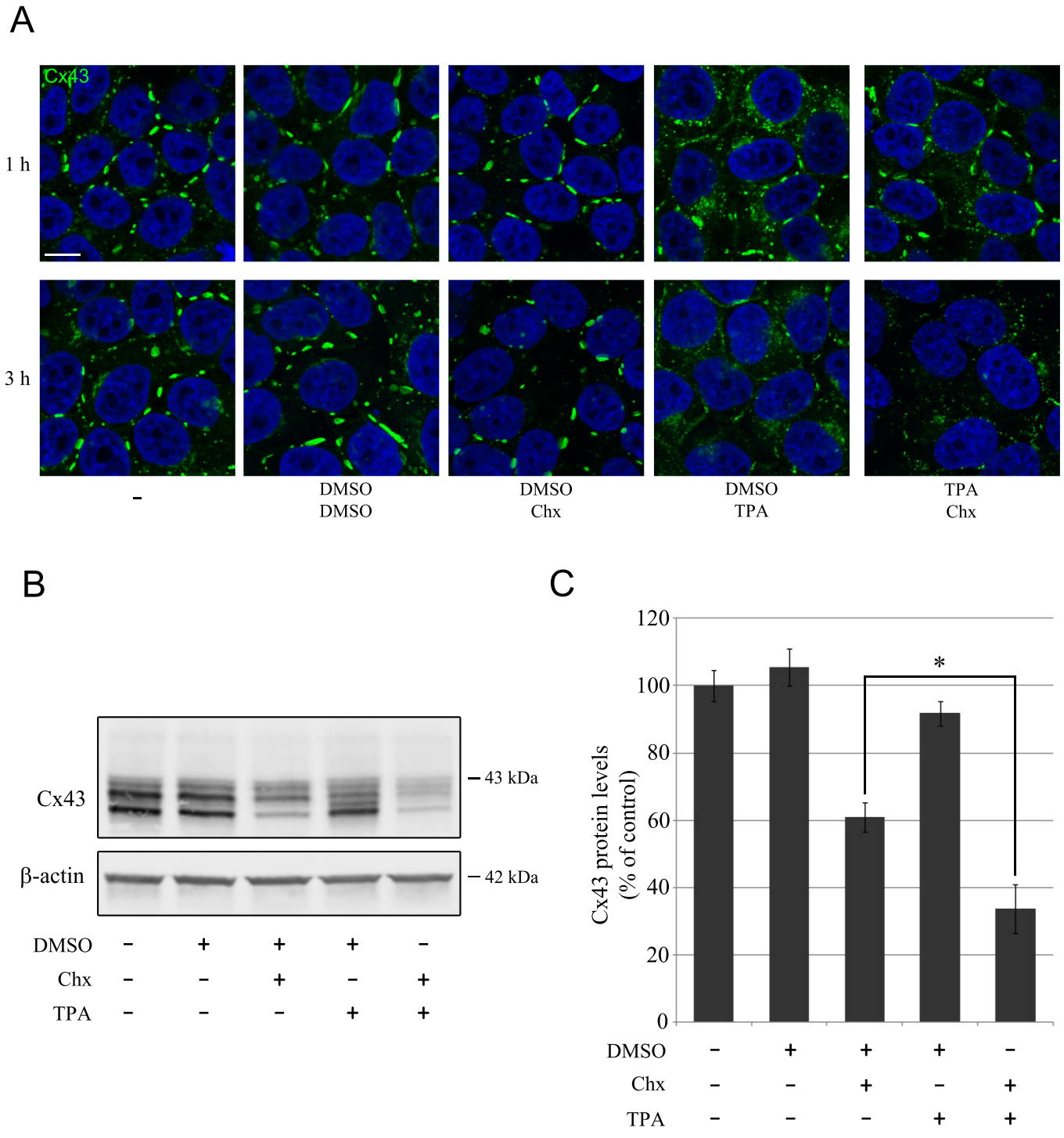

Supplementary Figure S6. Effect of TPA, Chx and DMSO gap junctions and Cx43 protein levels in HeLa-Cx43 cells. (A) HeLa-Cx43 cells were either left untreated, or treated with different combinations of TPA (100 ng/ml), Chx (10 µM) and DMSO (solvent) for 1 or 3 hours, as indicated. Cx43 (green) was then visualized by confocal fluorescence microscopy. Scale bar, 10 µm, applies to all images **(B)** HeLa-Cx43 cells were either left untreated, or treated with combinations of TPA (100 ng/ml), Chx (10 µM) and DMSO (solvent), in a similar manner as in A, for 3 hours. Cell lysates were then prepared, and equal amounts were subjected to SDS-PAGE. Cx43 and β-actin were detected by western blotting. Molecular mass in kDa is indicated. **(C)** The intensities of the Cx43 bands in B were quantified and normalized to the level of β-actin. Values shown are the means ± S.E.M. of three independent experiments. *$p<0.05$

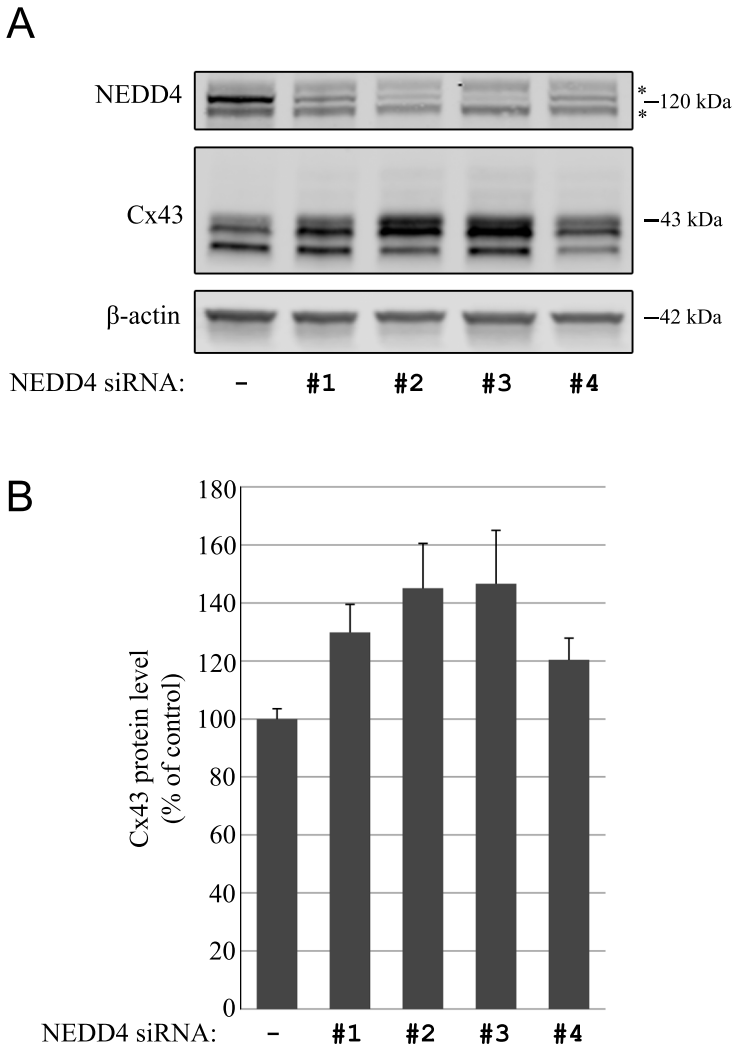

Supplementary Figure S7. Effect of siRNA-mediated depletion of NEDD4 on Cx43 protein levels. HeLa-Cx43 cells were transfected with control siRNA or with four different siRNA sequences against NEDD4. Cell lysates were prepared 96 hours after transfection, and equal amounts of total cell protein lysates were subjected to SDS-PAGE. NEDD4 and Cx43 were detected by western blotting using antibodies against NEDD4 and Cx43, respectively **(A)**. The membranes were also probed with antibodies against β-actin as a gel-loading control. The intensities of the Cx43 bands on western blots were quantified and normalized to the β-actin level **(B)**. Asterisks indicate unspecific bands. Values shown are the mean ± S.E.M of three independent experiments. Molecular mass in kDa is indicated.

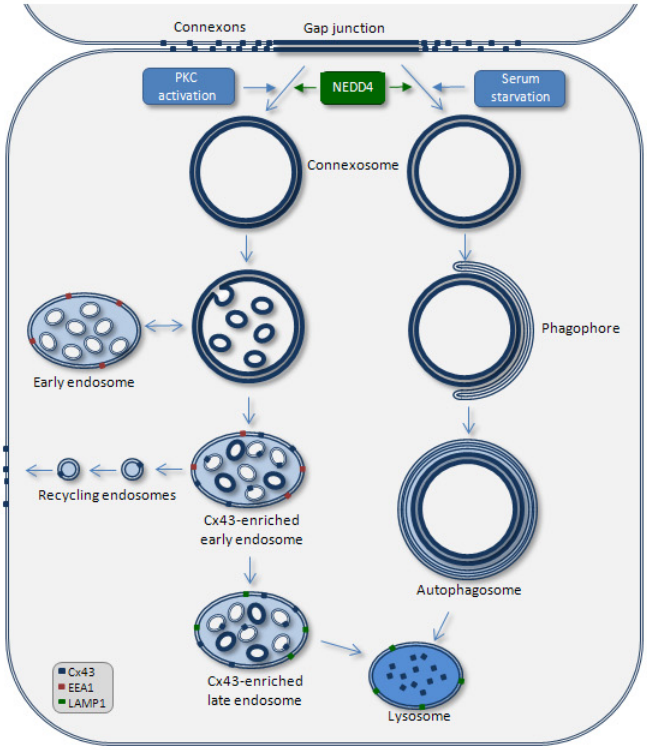

Supplementary Figure S8. Model of the role of NEDD4 in sorting of Cx43 from the plasma membrane to lysosomes. On the basis of the present and previous studies from our laboratory and other laboratories, we propose a model in which Cx43 is able to follow two distinct pathways en route to lysosomes following gap junction internalization. In the first pathway, connexosomes (i.e. annular gap junctions) undergo fusion with early endosomes. This fusion process is associated with the transformation of the connexosome from a double-membrane vacuole to a Cx43-enriched multivesicular endosome, which will eventually fuse with a lysosome. In the second pathway, connexosomes are enclosed by a phagophore, resulting in the formation of an autophagosome, which subsequently fuses with a lysosome. In this model, both pathways are involved in the degradation of Cx43 under basal conditions, and their relative importance is likely to differ between different cell types. Furthermore, the degradation of Cx43 along each of these pathways may be affected differently in response to changes in the intracellular or extracellular environments. For instance, activation of PKC promotes endocytosis and degradation of Cx43 along the endolysosomal pathway. On the other hand, serum starvation induces endocytosis and degradation of Cx43 along the autophagosomal pathway. Both the PKC- and serum-starvation-induced degradation of Cx43 are associated with increased Cx43 ubiquitination. Furthermore, NEDD4 is involved in both the PKC-induced degradation of Cx43 along the endolysosomal pathway and the serum-starvation induced degradation of Cx43 along the autophagosomal pathway.